3 MATERIALS AND METHODS

The methodology adopted for the investigation entitled **"Investigation of Biomass Derived Functional Carbon Electrodes from leaves of *Spathodea campanulata* and *Tecoma capensis* for Supercapacitor applications"** is discussed under the following phases.

Phase I: Synthesis of carbon materials (SPL/TCL) and nitrogen doped carbon from *Spathodea campanulata* and *Tecoma capensis* (SN/TN) Leaves

Phase II: Physiochemical and Morphological characterization of synthesized carbon materials-SPL/TCL/SN/TN

Phase III: Electrochemical characterization of SPL/TCL/SN/TN derived carbon materials for utilization of synthesized carbon materials in supercapacitor electrode applications

3.1. Reason for the selection of the waste biomass precursors

In this study, the waste plant leaves were used as biomass for the conversion of biomass carbon materials by considering the following reasons,

- ✓ Renewable and Sustainable Resource
- ✓ Waste Reduction and Recycling
- ✓ Cost-Effectiveness
- ✓ Environmental Benefits
- ✓ Local Availability
- ✓ Versatility

3.2. Materials

The fallen leaves of *Spathodea campanulata* (SPL) and *Tecoma Capensis* (TCL) were collected and powdered. This was utilised for synthesis. Analytically pure urea from Sigma- Aldrich (99%), Hydrochloric acid analytical reagent (AR) grade, with a minimum assay of ≥ 99% and pure absolute ethanol has been used.

3.3. Phase: I

Synthesis of Carbon Materials (SPL/TCL) and nitrogen doped carbon from *Spathodea campanulata* and *Tecoma capensis* (SN/TN) Leaves

3.3.1 Synthesis of Biomass carbon

The selected biomass precursors of *Spathodea campanulata* (SPL) and *Tecoma Capensis* leaves (TCL) were synthesized by direct pyrolysis method followed by carbonization process without any external activation. They were authenticated by the Botanical Survey of India and a voucher specimen was deposited (BSI/SRC/5/23/2022/Tech/496) (BSI/SRC/5/23/2022/Tech/497).

The waste leaves of SPL and TCL were collected in large quantity from nearby farm, Coimbatore, Tamilnadu, India. The collected leaves of SPL and TCL were cleaned well with tap water followed by distilled water to remove all the extraneous matter such as dust particles, impurities etc... The washed leaves were shade dried at room temperature. The shade dried leaves were ground to a fine powder using agate mortar. The powdered samples were then dried in oven at 80°C for 24 hours.

From the TGA analysis of Biomass precursors SPL/TCL), the mass loss of each sample was monitored until constant mass was achieved, at the temperature 105 °C, the mass loss occurred due to removal of moisture and the mass loss occurred at 500°C is due to combust organic components. Analysing the thermogravimetric (TG) curve of biomass allows identification of critical decomposition stages and temperature ranges where substantial mass loss occurs. This analysis also aids in choosing suitable pyrolysis temperatures (700,800,900°C), ensuring that biomass is properly processed without encountering undesired side reactions **(Lugo *et al.*, 2018)**. The TGA results have been presented in Chapter 4.

10g of collected dry leaves of *Spathodea campanulata* and *Tecoma capensis* were subjected to direct pyrolysis in an alumina crucible in a tubular furnace under nitrogen atmosphere. The pyrolysis was conducted at temperatures of 700°C, 800°C, and 900°C for a duration of three hours. Subsequently, the resulting carbonized solid was subjected to washing with 5M HCl and dried at 60°C overnight. Nearly 8g of carbonized materials were

obtained at different temperatures and designated as SPL-700, SPL-800, SPL-900, TCL-700, TCL-800, and TCL-900 respectively **(Biswal *et al*., 2013)**.

3.3.2: Synthesis of N-doped carbon from synthesised biomass carbon

The as-prepared carbon material (SPL-700, SPL-800, SPL-900, TCL-700, TCL-800, and TCL-900) was mixed with urea in the ratio of 3:1 (Urea: carbon) to facilitate nitrogen (N) incorporation into the carbon materials. Urea served as the nitrogen source in the carbon materials. The mixture was thoroughly homogenized at ambient conditions with intermittent stirring over a period of 12 hours. The crucible, containing the prepared mixture, was then placed in a tubular furnace and subjected to three different activation temperatures: 700°C, 800°C, and 900°C, with a heating rate of 5°C/min, under an inert atmosphere for 2 hours to initiate the doping process in the carbon materials. Following doping, the resultant mixture was washed repeatedly with deionized water to remove any residual impurities and maintain a neutral pH. The washed sample was then dried in a hot air oven at 60°C overnight to ensure complete drying. Nearly 2g of doped material was obtained and designated as SN-700, SN-800, SN-900, TN-700, TN-800, TN-900 **(Anitha *et al*., 2016)**.

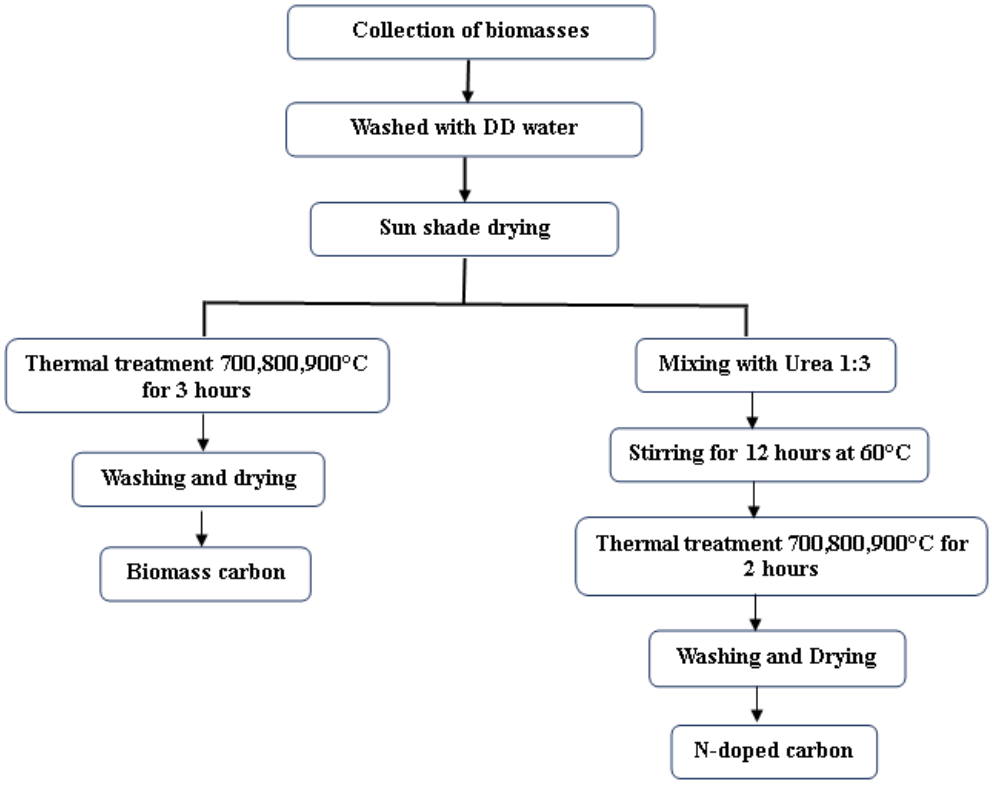

Figure 3.1: Synthesis of biomass and N-doped carbon

3.4. Phase: II

Physiochemical and Morphological characterization of synthesized carbon materials-SPL/TCL/SN/TN

3.4.1 Physiochemical Characterization

FT- IR: To determine the surface environment that resides in the carbon material, FT-IR spectroscopy was used. A FT-IR analysis has been carried out to determine the functional groups present in the prepared functional materials of SPL and TCL from chosen biomass. Using the **NICOLET iS10 spectrometer model**, the FT-IR spectra was captured at frequencies between 4000 and 500 cm^{-1}.

XRD: To understand the fundamentals about the structure of carbon material, the XRD spectrum was recorded. The XRD technique with the range of 10-90° utilizing an **XPERT-PRO Model** X-ray Diffractometer with Cu K radiation at step size 0.01-0.02°/ min has been used to examine the synthesized functional carbon materials of SPL, TCL from selected biomass. Using Scherrer formula, the crystallite size was found.

$$\mathbf{DP = (0.04 \times l) / (\beta \times \cos \theta) \rightarrow 1}$$

RAMAN Spectroscopy: The degree of graphitization of carbon material was assessed using Raman spectroscopy. Raman analysis has been used to investigate the TCL/SPL functional carbon material from the chosen biomass. Using the **JY Horiba Lab RAM HR 520**, the Raman spectrum with a range of 100-1000 cm^{-1} was acquired.3.4.2. Using Tuinstra Koenig Relation, the crystallite size was found.

$$\mathbf{La\ (nm) = (2.4 \times 10\text{-}10)\ \lambda 4\ (I_D/I_G)^{-1} \rightarrow 2}$$

3.4.2 Morphological-Compositional Analysis

FE SEM: By employing FE-SEM examination with a **Yes Carl Zeiss, the UK,** with an acceleration voltage of 15kV at various magnifications, the synthesized functional carbon material of SPL/TCL/SN/TN from selected biomass has been studied.

EDAX: The elements that were predicted to be in the carbon sample were obtained from EDS Spectroscopy. Using **Bruker Nano GmbH Berlin**, Germany, EDS spectra were taken

to determine the carbon content and other small traces in the functional carbon materials of TCL/SPL that were synthesized from chosen biomass (Esprit 1.9).

TEM: To learn clearly about the nanometric pores that are present in the carbon material, TEM analysis was examined. Using **FEI Tecnai G2** with an acceleration voltage of 120 kV, TEM images of selected biomass have been focused on the functional carbon material of SPL/TCL/SN/TN.

BET Surface Analysis: The surface area, isotherm type, and porosity of the carbon precursors were investigated using BET analysis. Utilizing **ASiQwin Quantachrome** Instruments, functional carbon compounds of SPL/TN were analysed using BET (Version.3)

3.5 Phase III

Electrochemical characterization of SPL/TCL/SN/TN derived carbon materials for utilization of synthesized carbon materials in supercapacitor electrode applications

Biomass carbon and N-doped carbon samples synthesized at different temperatures, were subjected to a comprehensive array of electrochemical characterization techniques aimed at evaluating their electrochemical properties.

The electrochemical characterization techniques employed include Cyclic Voltammetry (CV), Electrochemical Impedance Spectroscopy (EIS), Galvanostatic Charge-Discharge cycling. These techniques enable the investigation of various electrochemical features, such as the redox behaviour, charge storage capacity, capacitance, charge transfer kinetics, and stability of the biomass carbon and N-doped carbon samples.

3.5.1 Electrode Fabrication

To investigate the electrochemical, the synthesized functional carbon electrode materials were fabricated by using active materials, carbon black as carbon conductive additive and poly vinylidene fluoride (PVDF) used as binder in ratio of 80:15:5 dissolved in NMP solvent. After ensuring well dispersion, the slurry was coated on the graphene sheet with the surface area of $1cm^2$. The coated slurry was dried in oven (vacuum) 100°C for overnight. 1M H_2SO_4 used as the electrolyte in the three-electrode system. For three-electrode configurations, synthesized carbon electrode active material, saturated calomel

electrode (SCE) and platinum used as a working electrode, reference electrode and counter electrode respectively. Electrochemical studies (EIS, CV and GCD) were performed with **CH Instrument Model CHI660a** in a three-electrode configuration using the graphene sheet coated with the active material of about 1 mg.

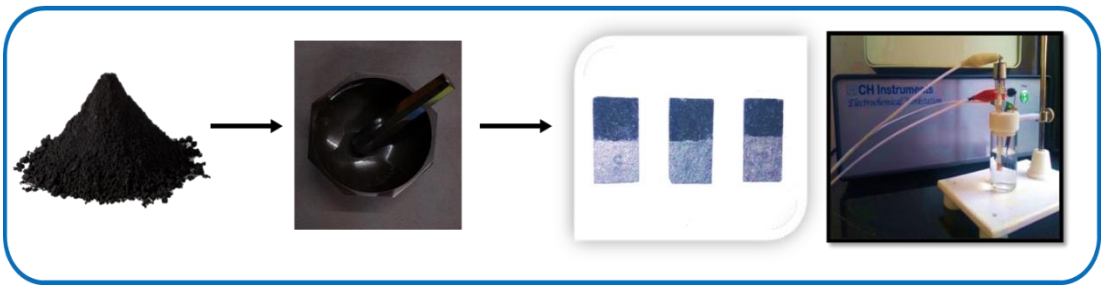

Figure 3.2: Electrode fabrication process for prepared carbon materials

3.5.2. Cyclic Voltammetry

Cyclic voltammetry is commonly employed to investigate the electrochemical properties of an analyte in solution. The potential is measured between the reference electrode and the working electrode, while the current is measured between the working electrode and the counter electrode. This data is then graphed as current (I) versus potential (E). As demonstrated by the waveform, the forward scan exhibits a current peak for analytes that can undergo reduction or oxidation (depending on the initial scan direction) within the scanned potential range. The current increases as the potential approaches the reduction potential of the analyte, but then diminishes as the analyte concentration near the electrode surface becomes depleted. If the redox couple is reversible, the applied potential is reversed, leading to the reoxidation of the product formed in the initial reduction reaction. This results in a reverse-polarity current peak, which usually exhibits a similar shape to the reduction peak. These observations provide valuable information regarding the redox potential and electrochemical reaction rates of the compounds **(Pearse *et al.*, 2016, Foca *et al.*, 2007).**

While an ideal capacitor without resistance would yield a rectangular voltammogram shape, most actual supercapacitor voltammograms adopt a parallelogram shape with irregular peaks. Prominent peaks occurring within narrow voltage windows often indicate pseudocapacitive behaviour. Faster sweep rates correspond to charging and discharging at higher power levels. To illustrate the impact of power levels on the charging characteristics, multiple plots obtained at increasing sweep rates are often superimposed on

the same graph. Consequently, it becomes evident that capacitance decreases at higher frequencies. The specific capacitance was evaluated from the area of the CV in a potential range from -0.2 V to 0.3V at different scan rate of 10-50 mV s^{-1}. The specific capacitance of a material is calculated from CV using the formula

$$\boldsymbol{c} = \int \boldsymbol{IdV} / \boldsymbol{vmV}\ (\boldsymbol{F}/\boldsymbol{g}) \rightarrow 3$$

where, $\int IdV$ integral area of the curve (A.V) v -scan rate (mV/s), m-mass of the active material (g), V-potential window (V).

3.5.4. Galvanostatic Charge- Discharge:

The determination of the specific capacitance of the supercapacitor electrodes is also accomplished through the galvanostatic charge-discharge technique. In an ideal capacitor, the discharge curves manifest as linear throughout the entire potential range, displaying consistent slopes that signify ideal capacitive behaviour. Galvanostatic charge discharge experiments were performed in a similar setup as described above with a specific current density of 75-250 µA g^{-1} and between -0.2 to 0.3V. To calculate the specific capacitance of the electrode in a three-electrode configuration, the following equation is employed:

$$\mathbf{C\ (F/g) = I\ \Delta t/m\ \Delta V \rightarrow 4}$$

Here, I correspond to the current employed for charge-discharge, Δt represents the elapsed time for charge or discharge, m denotes the mass of the active electrode, and ΔV signifies the voltage interval during charge or discharge. The energy density (ED in Wh/kg) and power density (PD in W/kg) of the carbon materials were estimated using the following formulae (5) and (6) **(Byatarayappa, G *et al.*, 2021).**

$$\mathbf{ED = (Cs \times V^2) / (2 \times 3.6) \rightarrow 5}$$

$$\mathbf{PD = (ED \times 3600)/td \rightarrow 6}$$

In an effort to elucidate the capacitive behaviour attributed to the presence of carbon black as an additive, super capacitive investigations were conducted using carbon black in the selected electrolyte employed in this study. Our objective was to measure the extent to which carbon black contributes to the overall capacitance of the system. Upon thorough investigation of the experimental findings, it was determined that the observed capacitive contribution of carbon black was minimal or probably excluded.

3.5.2 Electrochemical Impedance Spectroscopy

Impedance spectroscopy is one of the inexpensive and straightforward yet efficient methods receiving a lot of attention within the materials as it allows investigating many aspects of complicated materials properties. Such a method provides an excellent option to assess the dynamics of component performance in the frequency domain.

In the impedance spectrum, the shape of an ideal capacitor is represented by a vertical straight line, which is displaced on the real axis by the equivalent series resistance (ESR). With decrease in frequency range, a supercapacitor shows an almost vertical straight line, shifted on the real axis with the ESR along with an equivalent distributed resistance EDR **(Negroiu *et al*., 2017).**

The impedance in a supercapacitor tends to have notable significance to the application. At lower frequency, reactance, due mainly to capacitance, attains its maximum value and appears to be an electrostatic capacitance. During this period, ions are able to diffuse across the pores properly giving rise to maximum usage of the electrode area and a contribution to the double layer. Also, the distributed resistance becomes unchanged at the same time to its peak.

The presence of a Warburg element W in impedance Nyquist plots clearly demonstrates the distortion of appearance of the line inclined at an angle of 45° caused by a relatively slow growth in the sweep frequency region. With the increasing frequency, the capacitance starts to decrease, which results in less ionic penetration inside the pores and thus charging and discharging cycles can only take place on the surface of the electrodes. Understanding these impedance characteristics and their frequency-dependent variations provides valuable insights into the behaviour and performance of supercapacitor cells, aiding in the optimization of their design and operation **(Harris *et al*., 2019)**. AC impedance measurements were taken with a superimposing AC voltage of 5 mV within a frequency range of 1 MHz – 100 kHz **(Byatarayappa, G *et al.*, 2022).**

3.5.4. Fitting by software

Utilizing the EC-Lab software, the obtained impedance data for all the as-prepared materials have been fitted, and corresponding equivalent circuits of each three-electrode system is generated. These equivalent circuits are given in the corresponding result and

discussions sections. The software performed for the present study are Origin 2024 and EC-LAB Software V 10.37 version

3.8. Overall Framework for Methodology

Work plan carried out in the present study is depicted in the Figure 3.3

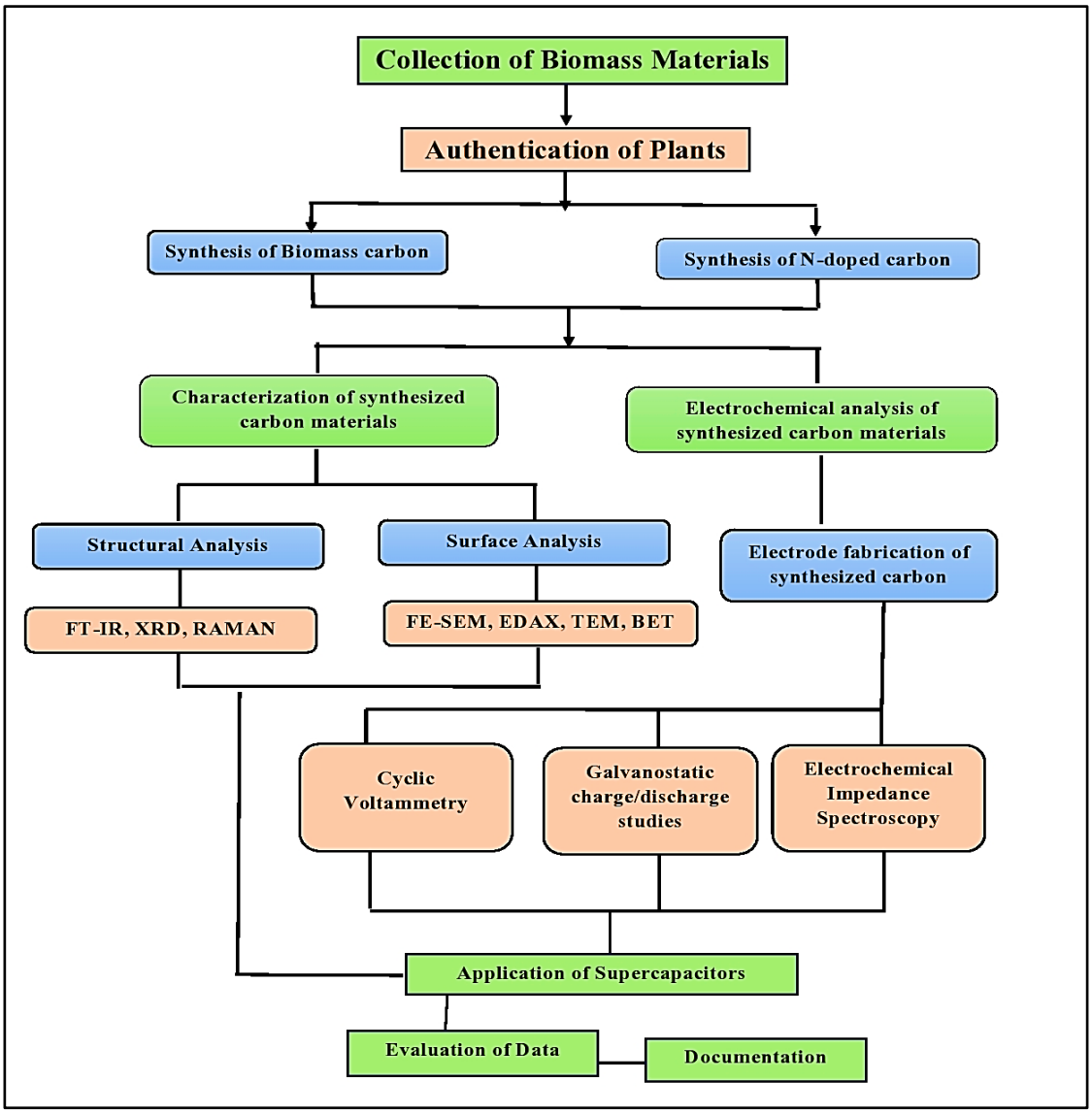

Figure 3.3: Overall framework for methodology

The results pertaining to the above framed methodology are discussed in chapter IV